ADVANCED SUSTAINABLE SYSTEMS
www.advsustainsys.com

Enhanced Nanocellulose Production from Cotton and Textile Waste Using Binary and Ternary Natural Deep Eutectic Solvents

Davud Karimian, Vincenzo Anzuoni, Zoe Smania, Laura Orian, Silvia Gross, and Mauro Carraro**

The growing accumulation of textile waste poses significant environmental challenges, as only a small percentage of materials is currently recycled. However, cotton waste offers a valuable feedstock for the regeneration of cellulose and nanocellulose (NC). This study presents a sustainable and efficient method for producing NC from textile waste using both binary and ternary natural deep eutectic solvents (NADESs). By treating cotton wool, pre-consumer standard cotton fabrics, and post-consumer denim textiles, with NADESs, NC generation is achieved in high yields (up to ≈90%) in all cases. The most promising NADESs, composed of choline chloride and gallic acid (and tartaric acid), effectively dissolve cotton-based materials when subjected to heating and sonication, producing cellulose nanocrystals with length ranging from 100 to 300 nm and crystallinity level up to ≈80%. The NADESs are characterized by thermogravimetric analysis (TGA), fourier transform infrared spectroscopy (FT-IR), as well as modeled by density functional theory (DFT), to investigate their hydrogen bond network. Eventually, their recyclability is also investigated. This approach opens promising applications in the fields of sustainable nanomaterial production and textile recycling, providing a greener alternative for waste valorization and promoting circular economy practices.

1. Introduction

The textile industry is steadily growing, resulting in the production and use of millions of garments annually, which significantly contributes to global water and resource consumption. The diverse activities of the textile sector, closely linked to the fashion industry, must meet the demands of ever-changing trends and new styles, leading to the generation of a large volume of textile products. However, the downside of this industry is the substantial production of waste, coupled with low recycling rates.[1,2]

There are essentially three types of textile waste: post-industrial, pre-consumer, and post-consumer. Post-industrial waste, originating from industries, typically consists of leftovers and scraps, which are readily traceable, compositionally homogeneous, and largely free of contaminants. Pre-consumer waste is similar to post-industrial waste but includes additional materials added for commercial purposes, such as joints, zippers, and buttons. Post-consumer waste is what remains after customer use. This type of waste is mostly contaminated and, depending on the extent of use, can be damaged, deformed, and is generally characterized by a complex, mixed, and heterogeneous composition.[3] For these reasons, it is also the most difficult type of textiles to sort, treat, and recycle. Among the waste textiles, denim fabrics represent a large fraction. It is estimated that 2.16 million tons waste denim, including pre and post-consumer material, are collected in Europe annually.[4]

To reduce the impact of these wastes and manage energy and raw material consumption, there is an urgent need to find green, sustainable, and cost-effective procedures to recycle textile waste or recover valuable materials for use in different production processes. In any case, separation procedures are fundamental, especially in the case of mixed textiles, and can be accomplished through selective processes involving solubilization, chemical transformation or degradation. Although many reports addressed this issue, most methods still involve expensive and toxic materials and/or harsh reaction conditions.[5–7] Concerning cotton, it can be treated to obtain regenerated cellulosic fibers for

D. Karimian, V. Anzuoni, Z. Smania, L. Orian, S. Gross, M. Carraro
Department of Chemical Sciences
University of Padova
Via F. Marzolo, 1, Padova 35131, Italy
E-mail: silvia.gross@unipd.it; mauro.carraro@unipd.it
S. Gross
Karlsruher Institut für Technologie (KIT)
Institut für Technische Chemie und Polymerchemie (ITCP)
Engesserstr. 20, 76131 Karlsruhe, Germany
M. Carraro
Institute on Membrane Technology (ITM)
UoS of Padova
National Research Council of Italy (CNR)
Via F. Marzolo, 1, Padova 35131, Italy

The ORCID identification number(s) for the author(s) of this article can be found under https://doi.org/10.1002/adsu.202400525

DOI: 10.1002/adsu.202400525

reuse in textile manufacturing or other cellulosic products. However, to recover non-modified cellulose, a suitable solubilization process is required. In particular, disrupting the hydrogen bond (HB) network within the cellulose structure, without degrading its polymeric chains, is still a major challenge and only few solvents as N-methylmorpholine N-oxide (NMMO) or ionic liquids (ILs) display such ability.[8,9]

Deep eutectic solvents (DESs) are a relatively new class of solvents, and have garnered significant interest in recent years. These solvents are primarily composed of two compounds that interact through hydrogen bonds and other weaker intermolecular forces. When mixed correctly, the hydrogen bond donor (HBD) and the hydrogen bond acceptor (HBA) form a hydrogen bond network, which reduces the lattice energy of the mixture. This interaction ultimately lowers the melting point of the mixture compared to that of the individual pure compounds.[10,11]

Since 2001, when Abbott et al.[12] introduced the concept, numerous hydrogen bond donors (HBDs) and hydrogen bond acceptors (HBAs) have been identified and extensively tested for DES formulations. While HBAs are predominantly from the quaternary ammonium family, a wider variety of compounds can be used as HBDs, including carboxylic acids, alcohols, and amines, as well as polar aromatic molecules.[14] A further subclass, known as natural deep eutectic solvents (NADESs), has been established to differentiate DES mixtures whose components are derived from natural sources, such as primary metabolites like amino acids, organic acids, sugars, or choline derivatives. These characteristic compositions result in biodegradability, biocompatibility, and renewability of the mixture.[15]

The increasing interest in using DESs for biomass treatment, has led to numerous reports showcasing their effectiveness in cellulose recovery and processing.[16] This has also encouraged the use of DESs as potential and versatile solvents for other cellulosic based materials.[17–21] A variety of HBD and HBA compounds were thus employed in the dissolution of cellulose or for the production of nanocellulose (NC).[22–32] Within this context, Table S1 in the Supporting Information provides a literature review comparing different DESs components and reaction conditions (ranging from thermal activation and microwave irradiation to sonication), which were tested for the extraction of nanocellulose (NC). Excellent yields, up to 95%, were achieved from various biomass sources, while the performance with virgin cotton fibers, in the explored conditions, was found to be 75%.[22]

Despite such valuable results, however, it is still evident the lack of a NADES capable of effectively interact with cotton-based materials, to dissolve cellulose and produce nanocellulose in high yield.

In this work, we have initially prepared a binary NADES based on an aromatic HBD and utilized it for separating the cellulose from textile waste and directly generate nanocellulose (NC) from dissolved cellulose. In particular, a NADES containing choline chloride (ChCl) as the HBA and gallic acid (GA) as the HBD was investigated (**Figure 1**). Gallic acid, or 3,4,5-trihydroxybenzoic acid, is a natural secondary metabolite that can not only be separated from many plants (such as spices, tea leaves, and oak bark),[33] but also produced in large quantities through biological and chemical synthesis. It has antioxidant properties and a unique structure, featuring a carboxylic acid group and three hydroxyl groups, which may form cooperative, directional, hydrogen bonds. This makes it an efficient compound for weakening the internal hydrogen bond network of cellulose, thereby facilitating its dissolution.[34] Beside the functional groups of gallic acid, that have an important role in the process of dissolving cellulose, the phenyl ring of this compound may also interact with cellulose, thereby restraining the aggregation of regenerated nanocellulose.[35]

Although this class of DESs with aromatic HBD has many capabilities, it has been scarcely investigated. Among the applications, treatment of lignin, wood delignification, and biomass pretreatment are the most focused ones.[36,37]

Ternary mixtures were also explored, assessing tartaric acid (TA) as the most promising additional component. TA is more acidic (pKa = 2.98) and cheaper than GA (pKa 4.41), thus representing a valuable additive to improve the cost-effectiveness of the resulting NADES (Figure 1).

To the best of our knowledge, this is the first time this NADES system has been used to generate nanocellulose, especially from textile waste.

2. Result and Discussion

2.1. DES for Cellulose Solubilization and Nanocellulose (NC) Production

An optimal DES composition, demonstrating good cellulose dissolution ability, should provide the acidic media to assist the cleavage of specific bonds in cellulose network.[38] Additionally, the presence of suitable functional groups plays a crucial role in establishing a HB network between the solvent and the solute, thereby weakening the cellulose's HB network and assisting its dissolution. Considering these key points, gallic acid, possessing a carboxylic and three phenolic groups, was selected as a suitable candidate for both tasks. As a second component of our devised DES, choline chloride, a well-known quaternary ammonium salt,[39] was used as HBA.

Since the effectiveness of the DES is closely related to their components' ratio, different molar ratios (ChCl:GA 1:2, 1:1.5, 1:1, 1.5:1, 2:1, 3:1) were explored, as summarized in **Table 1**. In the cases where higher ratios of GA were used, no eutectic mixture was observed, demonstrating that, in these molar ratios (1:1 ÷ 1:2), the interaction between the two components is not effective. Instead, by increasing the amount of ChCl with respect to gallic acid (1.5:1 ÷ 3:1), a pale yellow transparent homogenous liquid was obtained at 90 °C, suggesting that higher ChCl content may result in effective interplay of choline molecules with gallic acid and therefore, in a HB network strong enough to disrupt the one found within the pure components. When increasing the amount of ChCl, a correlation between its content and DES viscosity can be found. Besides, by using cotton wool as model cellulosic material, it was observed that the dissolution power of DES is also affected. Indeed, higher ChCl ratios (see 3:1 versus 2:1 ChCl:GA, molar ratio), although resulting in less viscous DES, decreased the apparent cellulose dissolution ability (Table 1). As a result, the 2:1 (ChCl:GA) formulation was chosen as the best one to be used for the dissolution of cellulose and NC preparation.

The nature of the DESs and of their HBD/HBA interaction was investigated through different analytical approaches. FT-IR spectra of gallic acid, choline chloride and of the resulting NADES are

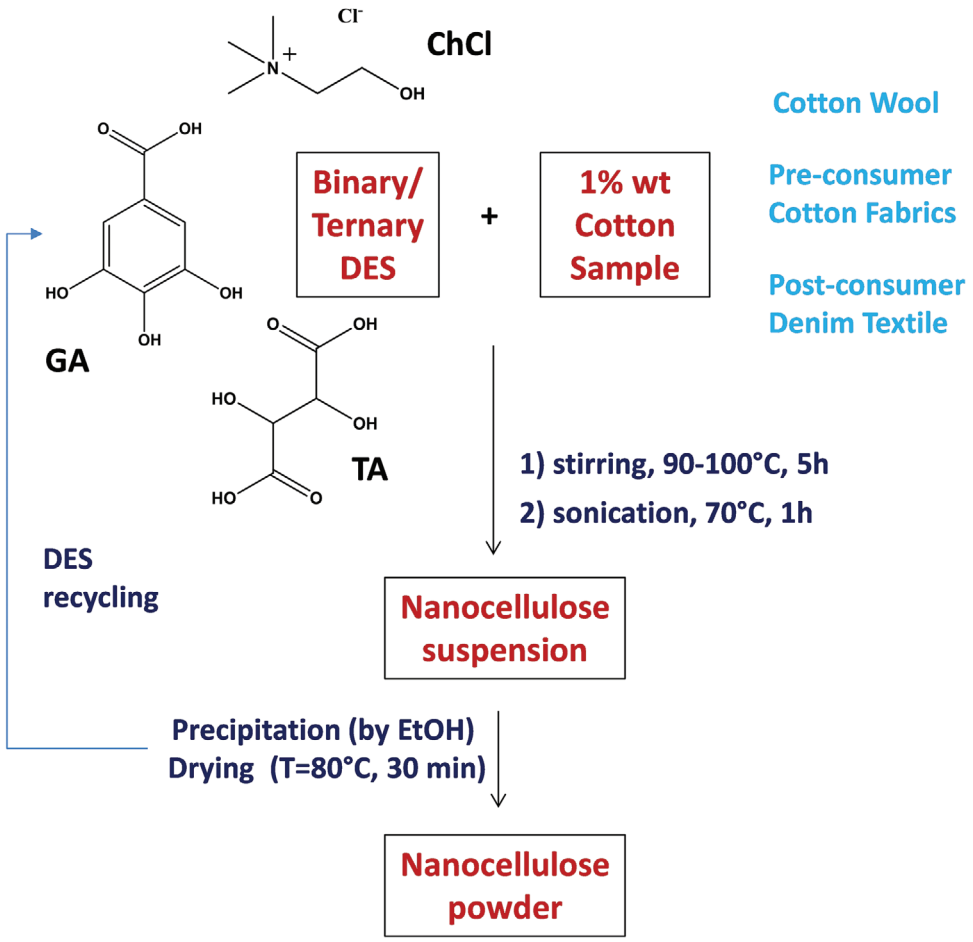

Figure 1. Process scheme for the production of nanocellulose from textile waste using NADES composed of choline chloride (ChCl), gallic acid (GA), and tartaric acid (TA).

depicted in Figures S1 and S2 (Supporting Information). DES spectra exhibit distinct peaks corresponding to both ChCl and GA. As observed, by increasing the amount of ChCl in the composition of NADES, the peaks around 620, 869, 954, 1033, 1449, 2905 and 3261 cm^{-1} show changes in intensity and minor variations in their wavenumbers.

Table 1. NADES formation based on different molar ratios of ChCl and GA.

ChCl [molar ratio]	GA [molar ratio]	NADES Formation	Output[a)]	Dissolving ability [% wt][b)]
1	2	✗	Powdery mixture	–
1	1.5	✗	Turbid mixture	–
1	1	✗	Turbid mixture	–
1.5	1	✓	Viscosity: 1.24 Pa•s	96
2	1	✓	Viscosity: 0.85 (Pa•s)	96
3	1	✓	Viscosity: 0.21 Pa•s	78

[a)] monitored at the temperature of the cellulose dissolution reaction (90 °C); [b)] calculated from the undissolved residue.

In the next step, the behavior of this NADES toward the generation of nanocellulose (NC) from waste textile was qualitatively investigated at different temperatures, in the range 70–120 °C (Table S2, Supporting Information). Between 70 and ≈85 °C, the solvent was not suitable to obtain NC: indeed, aggregation with formation of visible fiber-like residues was observed. Instead, between 85 and 100 °C, a successful production of high-quality (in terms of crystallinity and fibers morphology, see below) cellulose nanocrystals was achieved. It should be mentioned that, at higher temperatures (T = 120 °C), hydrolysis can occur to a greater extent, leading to damage of the recovered cellulose. Gathering all above information, we chose the 90 °C as the best temperature for operating the reaction. Regarding the thermal stability of the DES, the binary system remains stable in air up to 175 °C, as demonstrated by TGA (Figure S3, Supporting Information).

Various solute-to-solvent ratios were then employed to quantitatively evaluate dissolution effectiveness. According to **Table 2**, 0.5, 1, 2, and 3% wt. of cotton wool in NADES were studied. When the 0.5 or 1% cotton wool samples were prepared, a yellow solution was obtained after 4 h of stirring. The 2% cotton wool solution was more viscous than the 1% solution, making its use more difficult for further steps. Similarly, increasing the amount of cotton wool to 3%, led to only 62% dissolution with respect to the

Table 2. The yield of NC generation for cellulosic samples and in different conditions.

Entry	Sample	Conc. in DES [% wt.]	Conditions[a)]	Dissolving ability [% wt]	Generated NC [% wt]
1	Cotton wool	0.5	Heating (4 h)	95	61.6
2	Cotton wool	1	Heating (4 h)	95	62.1
3	Cotton wool	2	Heating (4 h)	89	58.7
4	Cotton wool	3	Heating (4 h)	62	–
5	Cotton wool	1	Heating (8 h)	96	67.4
6	Cotton wool	1	Heating + Sonication	96	88.5
7	Cotton Fabric	1	Heating + Sonication	95	85.1
8	Denim	1	Heating + Sonication	81	79.3

[a)] Operating conditions: DES volume 3 mL, heating at T = 90 °C, sonication for 1–2 h at 70 °C.

starting cotton weight, even with longer processing time. Due to such observation,1% wt. was chosen as suitable amount to proceed with the generation of nanocellulose from cotton sources.

As far as the process is concerned, in the initial step of the process, 1% wt. of the cotton sample was treated with NADES and stirred at 90 °C for several hours until the sample dissolved, resulting in a solution. By adding ethanol as a non-solvent to the solution, precipitation of cellulose was achieved. After centrifugation, separation and drying, the obtained cellulose was weighted and characterized. In Figure 1, the NC generation process using the selected NADES is summarized.

The dissolution progress was monitored at various heating steps. It was noticed that NADES required 4 h of stirring at 90 °C to dissolve the cellulose. Running the reaction for longer time provided a slightly higher yield of NC but, considering the time of the reaction and energy consumption issues, this is likely less convenient (Table 2, entry #5).

Following a different approach, the same heating step was performed and the mixture of cotton wool and NADES was heated until a solution was achieved. After this step, the mixture was sonicated for 1 h, finely suspending the cellulose nanocrystals, and resulting in a less viscose and darker solution. The rest of the procedure was the same and the generated NC obtained with this procedure was characterized. A higher yield of NC generation for the second route, involving sonication, was observed (entry #6 in Table 2). As a matter of fact, sonication can effectively help break down the cellulosic chains into shorter segments, resulting in smaller NC fragments.[22]

To assess the system's effectiveness in separating high quality NC, two textile materials were tested in the same optimized conditions and compared with cotton wool, namely a pre-consumer, standard cotton fabric and a post-consumer denim textile. As expected, the cotton fabric sample behaved similarly to cotton wool, achieving a transparent solution within 4 h. After solubilization, the process was followed by sonication and precipitation with the addition of a non-solvent to recover the nanocellulose from the solution. Table 2 shows comparable yields for both cotton fabric and cotton wool samples.

In comparison with the former cotton samples, dissolution of denim textile was more challenging, so that some adjustments to the procedure were introduced. Denim is indeed a more complex textile, differing in weave, weight and color. Besides requiring a longer heating time, the amount of dissolved cellulose was lower for denim samples compared to the other cotton samples. Moreover, an increased aggregation was observed, making thus necessary an extension of the sonication time, up to 2 h, to minimize the aggregation of the fibrils. In this way, NC from denim was successfully isolated with good yield (see Table 2). Another notable advantage of this system is the significant sample decolorization. It was noted, indeed, that the generated NC was less colored in comparison with the starting material. Since removing the color of textile is another important issue in textile recycling, the potential of this solvent system to facilitate green production of color-free NC from denim sources is particularly appealing.

In the subsequent phase of the investigation, the system was implemented to include ternary NADES, to examine the impact of a further component on viscosity and performance. In this context, a portion of GA was substituted with different HBDs. It is assumed that the presence of an additional HBD alongside GA could influence the hydrogen bond network of the solvent, potentially altering both its viscosity and its ability to interact with cellulose. Accordingly, different ternary NADESs were prepared and evaluated for dissolution of textile wastes and generation of nanocellulose. H_2O, lactic acid, glycerol and tartaric acid were examined as additional HBD, replacing a corresponding molar amount of GA. Molar ratios of 4:1, 1:1, and 1:4 of GA and co-HBD were utilized. It was observed that the prepared ternary NADESs with molar ratio 1:1 and 1:4 of GA:co-HBD display lower viscosity than the binary NADES in which the HBD part contains only GA. On the contrary, for the ratio 4:1 (GA:co-HBD) no considerable changes in viscosity with respect to the binary NADES were observed. Due to the different extent of intermolecular interactions,[40] the ternary NADES exhibit reduced viscosity in comparison to binary NADES. Rheological studies show the viscosity of the binary NADES (ChCl/GA 2:1) and ternary NADES (ChCl/GA/TA 2:0.5:0.5) to be 0.80 and 0.58 Pa·s at 90 °C, respectively. The latter formulation was characterized by FT-IR (Figures S4 and S5, Supporting Information) and TGA (Figure S6, Supporting Information), showing the absence of reactions between the components and thermal stability up to 190 °C.

The ability to dissolve textile waste and generate nanocellulose was then investigated for the ternary NADESs. The results, collected in **Table 3**, for a fixed ratio of components (ChCl:HBD1:HBD2 = 2:0.5:0.5), showed that, among the different formulations of ternary NADESs, the one with tartaric acid is

Table 3. Dissolving ability and nanocellulose generation from cotton fabric by ternary NADES in a selected molar ratio.[a)]

Components	Molar ratio	Dissolving ability [% wt.]	Generated NC [% wt.]
ChCl / GA / H_2O	2 / 0.5 / 0.5	77	49.7
ChCl / GA / LA	2 / 0.5 / 0.5	89	64.1
ChCl / GA / Gly	2 / 0.5 / 0.5	70	57.4
ChCl / GA / TA	2 / 0.5 / 0.5	94	72.8

[a)] Reaction condition: DES volume 3 mL; heating 4 h, at 90 °C, sonication 1 h.

the best, with 94% dissolution ability and 73% NC yield from the standard cotton fabric. Although this NADES showed to be less performing than the binary DES containing only GA and ChCl (Table 2, entry 7), these findings show that efficiency and viscosity can still be carefully tailored to match the processing needs, also in view of a lower cost of TA.

For evaluating the potential of this solvent system, the recyclability of the aforementioned binary (ChCl:GA) and ternary (ChCl:GA:TA) DESs was examined. To this aim, after separating the DES from the generated NC, the residual solvent was heated to 80 °C to remove the ethanol and almost quantitatively recovered (76-95%) to be reused for dissolving cotton wool and for the production of NC. The results are collected in **Table 4** and show that both the binary and ternary DESs maintained their ability to produce NC in good yield even after three times of reusing. FTIR spectra for the fresh and reused DESs are shown in Figures S7 and S8 (Supporting Information), indicating the preservation of most bands.

2.2. Modeling of HBA/HBD Interactions

As described in the Introduction, the phase properties of DESs have molecular origin, rooted in intermolecular interactions characterized also by the presence of weak halogen and hydrogen bonding. We have thus investigated the nature of HBA (choline) and HBD (tartaric and gallic acids) interactions of the studied systems using molecular models and DFT calculations (see Computational details).

Table 4. Recyclability of NADES toward nanocellulose generation from cotton wool.[a)]

NADES	Recycle	NADES recovery [% wt.][b)]	Generated NC [% wt.]
ChCl:GA	Fresh	–	88.5
	1	91.1	85.4
	2	82.2	83.8
	3	75.6	82.4
ChCl:GA:TA	Fresh	–	84.8
	1	95.4	83.3
	2	86.4	81.6
	3	81.8	80.6

[a)] Reaction condition: DES volume 3 mL; heating 4 h, at 90 °C, sonication 1 h; [b)] recovered after separation and evaporation of ethanol at 80 °C.

Table 5. Energy Decomposition Analysis (EDA) results on the structures shown in Figure 2. All values are in kcal mol^{-1}. Level of theory: ZORA-M06/TZ2P.

	ΔE_{elstat}	ΔE_{OI}	ΔE_{Pauli}	ΔE_{int}
II-COOH	−22.39	−13.04	17.31	−18.12
II−OH	−27.4	−16.31	20.55	−23.16
2−II-a	−55.07	−36.22	44.42	−46.87
2−II-b	−41.39	−22.35	27.81	−35.94

First, two structures for choline were fully optimized at M06/6-311G(d,p) level of theory (Figure S9, Supporting Information), differing on the position of the chloride ion, which do not show significant energy difference. Then, the geometries of several adducts have been hypothesized and identified on the potential energy surface of the systems choline + tartaric acid (I) and choline + gallic acid (II). For I, without any stereoisomeric preference for the tartaric acid, we observed that the interaction with choline is established between the chloride anion and either the hydroxyl or the carboxylic proton. This latter is characterized by a shorter Cl—H distance, that is, 1.94 versus 2.19 Å, and by a much more negative Gibbs free energy of formation, that is, −14.40 versus −9.43 kcal mol^{-1} (Figure S10, Supporting Information). For II, the interactions via the carboxylic group (II-COOH) and via one hydroxyl group (II-OH) are characterized by a H—Cl distance of 2.05 and 2.07 Å, respectively (**Figure 2**A,B). Interestingly, in the adduct shown in Figure 2B, an H—O short distance is observed between the H atom of a second hydroxyl group of the gallic acid and the O atom of the hydroxyl group of choline. Overall, in terms of Gibbs free energy, the formation of II-OH is thermodynamically more favored than II-COOH, that is, −13.84 versus −12.53 kcal mol^{-1}.

We have then explored two adducts with two molecules of choline, in which the gallic acid is sandwiched between them (Figure 2C) and in which both cholines are arranged above the gallic acid (Figure 2D). In this latter case, choline-choline interactions are also allowed and the formation of this adduct is thermodynamically more favored, that is, −44.75 versus −25.13 kcal mol^{-1}, respectively. Insight on the nature of the interaction between the gallic acid and one/two choline molecules is provided by the calculation of the interaction energy and its decomposition (see Computational details).

In **Table 5**, the results are collected. In II-OH, the interaction between choline and the gallic acid is much stronger than in II-COOH. In fact, the slight increase in the Pauli repulsion, is counterbalanced by the largely more negative electrostatic and orbital interaction terms. Notably, when going from one to two choline molecules, the interaction become much stronger, supporting the experimental evidence of this favorable stoichiometry. In particular, the interaction is much larger when the gallic acid is sandwiched between the cholines (2-II-a).

In 2-II-b, (Figure 2D) choline-choline interactions are present, and the Pauli repulsion is closer to that computed for II-OH (Figure 2B), but the much more negative electrostatic and orbital interaction contributions justify the significant total interaction energy. Interestingly, all adducts between ChCl and GA still have free OH, available for the interaction with cellulose.

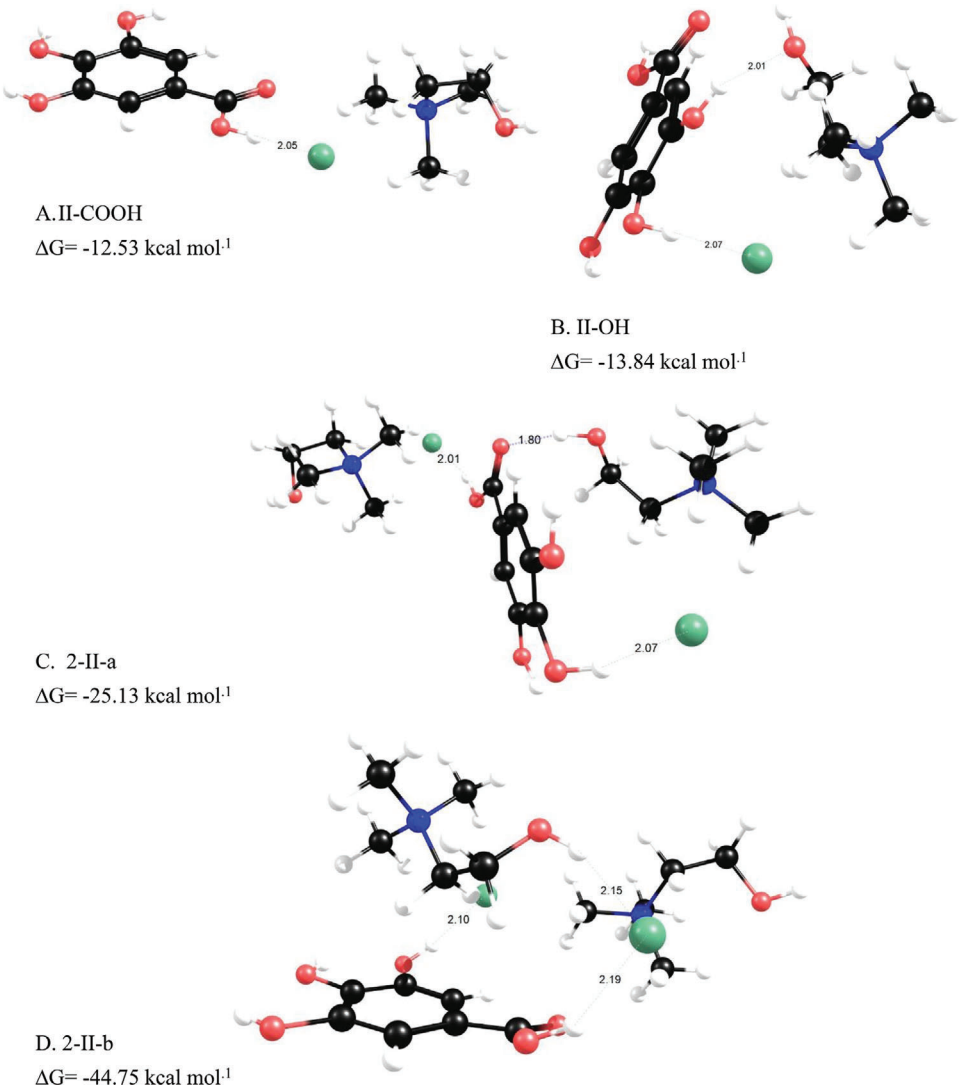

Figure 2. Optimized molecular structures of different adducts of II and 2-II. Level of theory: M06/6-311G(d,p).

2.3. Nanocellulose Characterization

After processing, the obtained NC was characterized through various techniques. **Figure 3** (and Figure S11, Supporting Information) shows the FT-IR spectra of nanocellulose generated from cotton fabric and denim sample, which were compared with pure cellulose spectrum. The peaks at 1670, 1425, 1375, 1160, 1115, 1060, and 895 cm^{-1} are related to the characteristic peaks of the cellulose,[17] and could be observed in all spectra. Interestingly, peaks ascribed to ester formation, resulting from the possible reaction between carboxylic groups of the organic acids with hydroxyl groups of cellulose, were not detected.

The crystal structure and crystallinity index (CrI)[41] of the recovered NC were studied thorough X-Ray diffraction (XRD). As can be seen in **Figure 4**, the XRD diffractograms of generated NC and raw cellulose present the same pattern and the main Bragg peaks (2θ = 14.6°, 16.6° and 22.6°) are observable for the three samples.

This proves that generated NC crystals have the same crystal structure as cellulose. Considering that the sample processing implies a modification in the amorphous/crystalline domains ratio within the polymeric chain of cellulose, further evaluation of NC was achieved by calculating the crystallinity index (CrI). The obtained results showed that the CrI for NC from CF is 79.5%, while for NC generated from denim is 78.2%. In comparison, raw cotton has a CrI of 64.9%. Thus, the overall crystallinity increased by 17–19% after the treatment, a result in agreement with the assumption that hydrolysis occurs preferentially in the amorphous domains.

The thermal stability of the generated NC from cotton fabric and denim was investigated by TGA analysis. The main decomposition was observed at ≈318 °C for NC from CF and 310 °C for NC from denim (**Figure 5**). In comparison, raw cotton has a degradation offset at 300 °C,[42] thus, the generated NC shows a slightly higher thermal stability, as a consequence of the removal of amorphous domains.[43]

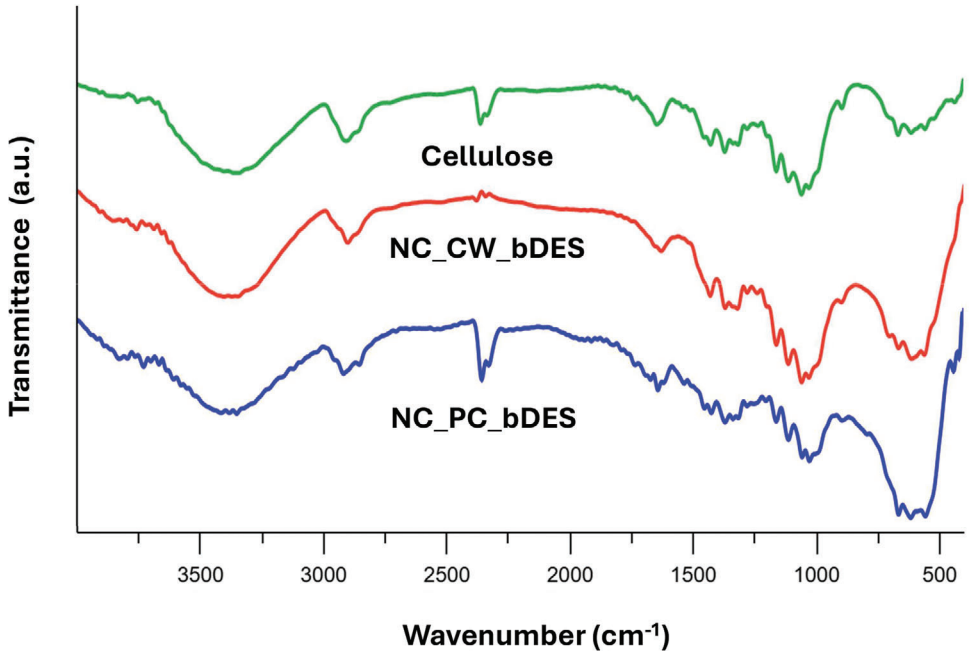

Figure 3. The FT-IR spectra of generated NC from cotton wool (CW) and post-consumer (PC) samples, by the binary DES (bDES), in comparison with cellulose.

The nanometric size of the nanocellulose was confirmed through TEM microscopy, as shown in **Figure 6**. The length of the NC fibers was found in the range 100–300 nm, with diameters 10–15 nm. Transmission electron microscopy (TEM) and scanning transmission electron microscopy (STEM) images of nanocellulose obtained from treatment of denim wastes with ternary NADES are also shown in Figures S12 and S13 (Supporting Information), respectively.

The natural-based DESs presented in this work showed to be adequate solvents to achieve dissolution and, consequentially, to pursue separation of cellulose from textile waste. This method, compliant with many of the green chemistry principles, proved to be effective with different kinds of cotton-based materials, where the NADES can effectively react with the cellulose network and turn it into nano-sized cellulose with appreciable yield and high crystallinity.

3. Conclusion

This study, for the first time, presents a green, straightforward, and efficient way to generate nanocellulose from textile waste. A natural-based DES (NADES) was synthesized using choline chloride and gallic acid with molar ratio of 2:1, which showed the best properties in terms of thermodynamic stability and solubilization performance. This powerful solvent succeeded to effectively dissolve different kinds of cotton sources.

The presence of carboxylic acid and hydroxyl groups in the HBD component of NADES provides acidic media and fosters an efficient interaction with cellulose. These functional groups, indeed, establish new hydrogen bonds network between solvent components, while leaving further sites to interact with cellulose, which led to dissolving cellulosic samples. Using synergically sonication process along with heating helped to disintegrate cellulose and increased the percentage of nanocellulose generation up to 89%. Also, through this method the crystallinity of the recovered materials had an increase of 20%. As a result, we employed a natural-based solvent not only for the separation of cellulose but also for optimizing a novel and effective method to valorize textile waste by generating nanocellulose.

In conclusion, our investigation aims to expand the potential applications of NADESs, not only for sustainable biomass processing (such as the solubilization of lignocellulosic materials or the extraction of biomolecules and metabolites) but also for the treatment of waste cotton materials. Future research will focus on clarifying the interactions between NADES and cellulose structures, while broadening the variety of starting cellulosic materials, to include more complex textiles, and optimizing the recycling process of DESs, within a full circular economy perspective.

4. Experimental Section

Materials and Chemicals: Gallic acid, choline chloride, lactic acid, tartaric acid, glycerol, and ethanol were purchased from Sigma–Aldrich. A commercial medical grade cotton wool was used in the reactions. Cotton textiles were sorted into pre-consumer and post-consumer fabrics, excluding those with synthetic fibers. Post-consumer denim was subjected to laundry washing prior to use. Both fabrics were cut in small pieces (1×1 cm^2) and shredded. FTIR spectra were recorded, preparing KBr pellets, on JASCO 4100 or Agilent Cary 630 FTIR instruments, from 400 to 4000 cm^{-1} in transmittance mode, with a resolution of 4 cm^{-1}. TGA were performed on a TA with the following T program: 50 °C × 10 min, 20 °C min^{-1} up to 700 °C, under air or nitrogen. Powder X-ray diffraction (XRD) patterns were collected by a Bruker AXS D8 instrument, using Cu anode powered with 40 kV and a current of 40 mA and scanning rate of 4° min^{-1}. TEM images were obtained by FEI Tecnai G^2 microscope operating at 100 kW, after dispersion in water and sonication of the samples. Samples were stained with Uranyl acetate prior to analysis. A TEM JEOL F200 was

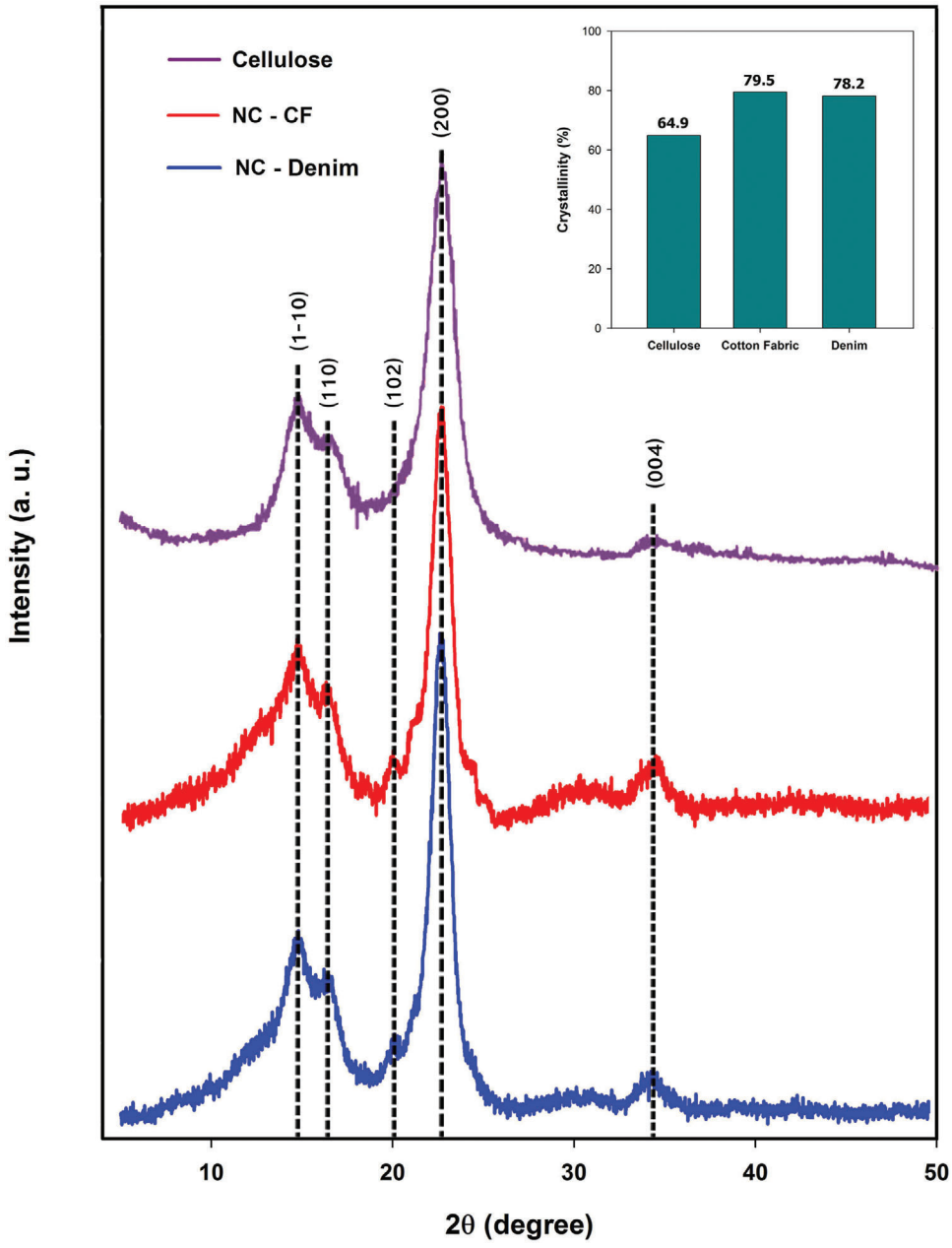

Figure 4. XRD patterns for generated NC from pre-consumer cotton fabric and post-consumer denim, in comparison with cellulose. The inset shows the increased crystallinity of generated NC from CF and denim. The observed peaks are located around 14.6°, 16.6°, 20.8°, 22.6°, and 34.2° and correspond to the crystalline planes of (1-10), (110), (102), (200), and (004), respectively.

used for STEM analysis. Rheological analyses were carried on by KINEXUS Lab+ rotational rheometer. A plate/plate geometry (20 mm) with the fixed gap of 0.3 mm was employed. The instrument INSEIS PT 1000 was used for TGA analysis. The products were recovered upon centrifugation by a HERMLE Z 32 HK centrifuge operating at 10 000 rpm. A sonicator ARGO LAB AU-65 was used to operate the dissolution process and to disperse the samples.

Computational Details: Full geometry optimizations were performed in gas-phase using M06 potential, a meta-hybrid functional with 27% HF exchange,[44] combined with 6–31G(d,p) basis set for all the atoms, as implemented in Gaussian16.[45] Frequency calculations were carried out at the same level of theory (M06/6-311G(d,p)) in order to confirm the stationary points (all positive frequencies) and to compute the thermodynamic corrections at 298 K and 1 atm. The stability of the different HBD/HBA systems tartaric acid + choline (I) and gallic acid + choline has been evaluated in terms of their Gibbs free energy of formation, that is, by subtracting to the total energy, the Gibbs free energies of the fully optimized individual components (tartaric/gallic acid and choline). Each system was then partitioned into two fragments, that is, choline and gallic acid one/two molecules. The interaction energy was evaluated and decomposed according to the Energy Decomposition Analysis (EDA),[46] as implemented in the Amsterdam Density Functional (ADF) program 2019.307.[47] The M06[44]was selected combined with all electron TZ2P basis set; relativistic effect were treated with ZORA[48] (level of theory: ZORA-M06/TZ2P).

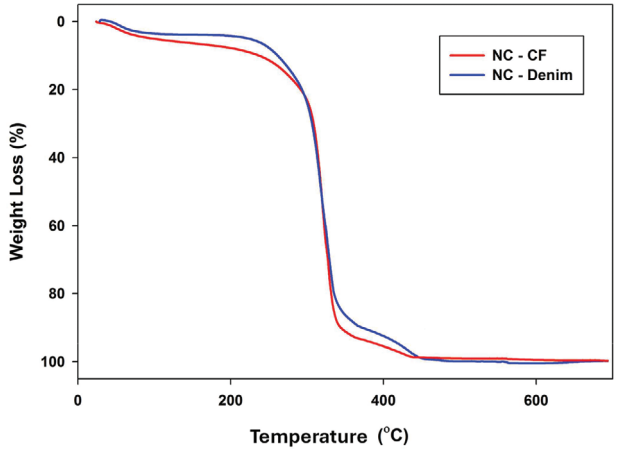

Figure 5. TGA curves collected under N_2, for generated NC from cotton fabric (CF) and denim in treatment with binary NADES composed of ChCl:GA (2:1). Temperature program: 50 °C × 10 min, 20 °C min^{-1} up to 700 °C.

According to the EDA scheme, the interaction energy between the two chosen fragments can be split into different contributions:

$$\Delta E_{int} = \Delta E_{elstat} + \Delta E_{OI} + \Delta E_{Pauli} \quad (1)$$

where ΔE_{elstat} represents to the semiclassical electrostatic interaction between the unperturbed electron densities of the distorted fragments; ΔE_{OI} accounts for all the occupied-void orbital interactions, such as the HOMO-LUMO interaction, and ΔE_{Pauli} (Pauli or exchange repulsion) is related to the repulsion between occupied orbitals localized on the two fragments. This analysis provides interesting and intuitive quantitative justification of chemical bonding and interaction.[49]

Cartesian coordinates of the optimized molecular structures are provided in the Supporting information (Table S3).

NADES Preparation: For the synthesis of NADES with molar ratio of 2:1 (ChCl:GA), 0.02 mol choline chloride and 0.01 mol gallic acid were weighted and vigorously mixed for a few minutes. Then, the mixture was placed under stirring, in a closed vessel, at the temperature of 90° C. After 2 h, a transparent pale yellow liquid of desired DES was obtained. The NADESs with other ratios of components were prepared in a similar way. In order to maximize the effectiveness of the solvent, the NADESs were freshly synthesized and utilized. For the synthesis of ternary NADESs, the appropriate molar ratio of the compounds was weighted and the same procedure was followed.

NC Generation: In the treatment of NADES with cellulosic samples, 1% wt. of sample was slowly added to the stirring solution of NADES at 90° C. The speed of the stirring was gradually increased during the process. After 4 h, the mixture was cooled and the undissolved parts were separated by filtration. In the next step, the transparent viscous solution was put in the sonicator with mild heating. The sonication was continued for 1 h, then, 10 mL of ethanol were added slowly to the solution (≈3 mL), which was let under stirring overnight at room temperature. The fine particles of nanocellulose slowly precipitated during the stirring. The generated nanocellulose was centrifuged at 10 000 rpm for 10 min. After centrifugation, the supernatant was removed, and the product was washed three times with ethanol, to remove any remaining NADES residue, and dried under vacuum.

Recycling Test: For the recycling tests, after centrifuging of the mixture containing cotton wool treated with first-time-used NADES, the generated nanocellulose was separated by precipitation and the remaining liquid was taken out to be heated under stirring to remove the ethanol. Then, the obtained recycled NADES was used for the treatment of further cotton wool.

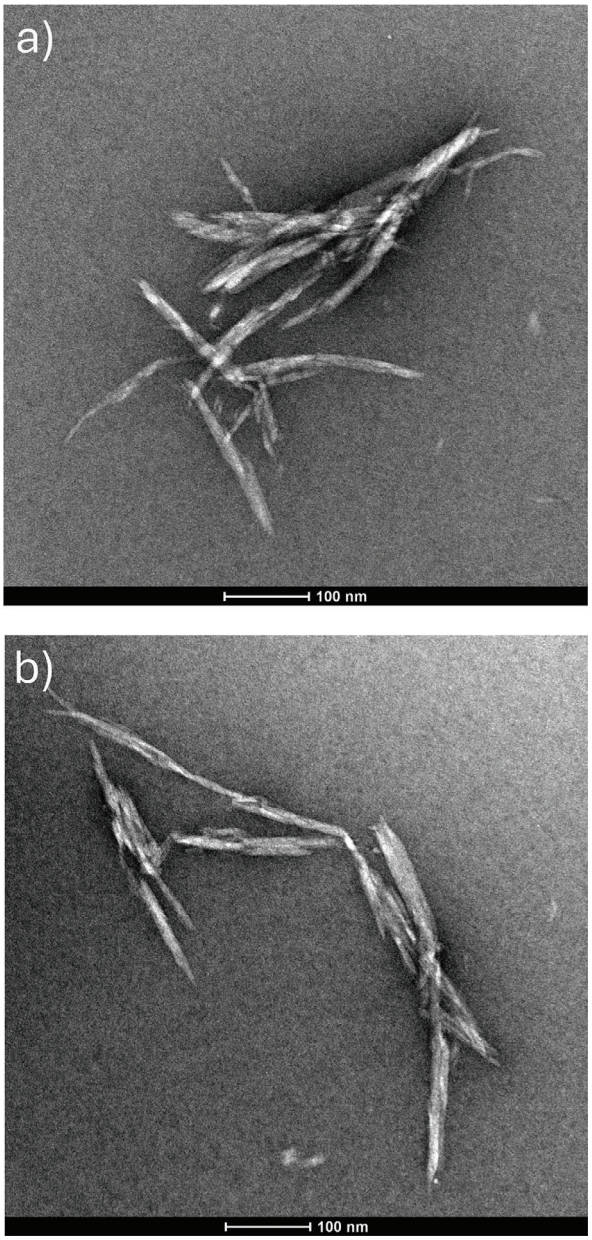

Figure 6. TEM images of generated nanocellulose from CF (a) and denim (b) samples treated with binary DES.

Supporting Information

Supporting Information is available from the Wiley Online Library or from the author.

Acknowledgements

This study was carried out within the MICS (Made in Italy – Circular and Sustainable) Extended Partnership and received funding from Next GenerationEU (Italian PNRR – M4 C2, Invest 1.3 – D.D. 1551.11-10-2022, PE00000004). The authors thank Prof. Maria Cristina Lavagnolo for project administration. Dr. Ilaria Fortunati for the kind assistance in the use of the Malvern rheometer, which was funded by the Fondazione CARIPARO within the InnoGel project (Progetti di Eccellenza 2017).

Open access publishing facilitated by Universita degli Studi di Padova, as part of the Wiley - CRUI-CARE agreement.

Conflict of Interest

The authors declare no conflict of interest.

Data Availability Statement

The data that support the findings of this study are available from the corresponding author upon reasonable request.

Keywords

cotton, deep eutectic solvents, nanocellulose, valorization, waste textiles

Received: July 22, 2024
Revised: September 26, 2024
Published online: October 16, 2024

[1] V. Amicarelli, C. Bux, M. P. Spinelli, G. Lagioia, *Waste Manag.* **2022**, *151*, 10.
[2] N. Norup, K. Pihl, A. Damgaard, C. Scheutz, *Waste Manag.* **2018**, *79*, 8.
[3] M. D. Stanescu, *Environ. Sci. Pollut. Res.* **2021**, *28*, 14253.
[4] A. Luiken, G. Bouwhuis, *Denim: Manufacture, Finishing and Applications*, Elsevier, Amsterdam New York **2015**, 527–612
[5] Y. Hu, C. Du, S. Y. Leu, H. Jing, X. Li, C. S. K. Lin, *Resour. Conserv. Recycl.* **2018**, *129*, 27.
[6] S. Yousef, M. Tatariants, M. Tichonovas, Z. Sarwar, I. Jonuskiene, L. Kliucininkas, *Resour. Conserv. Recycl.* **2019**, *145*, 359.
[7] I. Wojnowska, K. Bernat, M. Zaborowska, *Int. J. Environ. Res. Public Health.* **2022**, *19*, 5859.
[8] P. V. Barbara, A. A. Rafat, J. P. Hallett, A. Brandt-Talbot, *Curr. Opin. Green Sustain. Chem.* **2023**, *41*, 100783.
[9] S. Zhang, C. Chen, C. Duan, H. Hu, H. Li, J. Li, Y. Liu, X. Ma, J. Stavik, Y. Ni, *Bio. Res.* **2018**, *13*, 4577.
[10] E. L. Smith, A. P. Abbott, K. S. Ryder, *Chem. Rev.* **2014**, *114*, 11060.
[11] T. El Achkar, H. Greige-Gerges, S. Fourmentin, *Environ. Chem. Let.* **2021**, *19*, 3397.
[12] A. P. Abbott, G. Capper, D. L. Davies, H. L. Munro, R. K. Rasheed, V. Tambyrajah, *Chem. Commun.* **2001**, *19*, 2010.
[13] Y. L. Chen, X. Zhang, T. T. You, F. Xu, *Cellulose.* **2019**, *26*, 205.
[14] X. Li, K. Ho Row, *J. Sep. Sci.* **2016**, *39*, 3505.
[15] Y. Liu, J. B. Friesen, J. B. McAlpine, D. C. Lankin, S. N. Shen, G. F. Pauli, *J. Nat. Prod.* **2018**, *81*, 679.
[16] I. Bodachivskyi, C. J. Page, U. Kuzhiumparambil, S. F. R. Hinkley, I. M. Sims, D. Bradley, G. Williams, *ACS Sustain. Chem. Eng.* **2020**, *8*, 10142.
[17] H. Wang, J. Li, X. Zheng, X. Tang, Y. Sun, T. Lei, L. Lin, *Cellulose.* **2020**, *27*, 1301.
[18] J. Wang, Y. Wang, Z. Ma, L. Yan, *Green Energy Environ.* **2020**, *5*, 232.
[19] F. Shu, Y. Guo, L. Huang, M. Zhou, G. Zhang, H. Yu, J. Zhang, F. Yang, *Ind. Crop. Prod.* **2022**, *177*, 114404.
[20] J. Sonyeam, R. Chaipanya, S. Suksomboon, M. J. Khan, K. Amatariyakul, A. Wibowo, P. Posoknistakul, B. Charnnok, C. G. Liu, N. Laosiripojana, C. Sakdaronnarong, *Sci. Rep.* **2024**, *14*, 7550.
[21] W. Li, Y. Xue, M. He, J. Yan, L. A. Lucia, J. Chen, J. Yu, G. Yang, *Nanomaterials.* **2021**, *11*, 2778.
[22] Y. Liu, B. Guo, Q. Xia, J. Meng, W. Chen, S. Liu, Q. Wang, Y. Liu, J. Li, H. Yu, *ACS Sustain. Chem. Eng.* **2017**, *5*, 7623.
[23] J. Jiang, N. C. Carrillo-Enríquez, H. Oguzlu, X. Han, R. Bi, J. N. Saddler, R. C. Sun, F. Jiang, *Carbohydr. Polym.* **2020**, *247*, 116727.
[24] L. Douard, M. N. Belgacem, J. Bras, *ACS Sustain. Chem. Eng.* **2022**, *10*, 13017.
[25] Q. L. Lu, J. Wu, Y. Li, L. Li, B. Huang, *J. Mater. Sci.* **2021**, *56*, 12212.
[26] Y. Xu, Y. J. Xu, H. Chen, J. Xiong, M. Gao, *Wood Sci. Technol.* **2022**, *56*, 1761.
[27] X. Deng, L. Wan, H. Sun, C. Li, F. Liu, X. Yan, K. Liu, S. Ye, *Bio. Res.* **2022**, *17*, 714.
[28] X. Wu, Y. Yuan, S. Hong, J. Xiao, X. Li, H. Lian, *Ind. Crops Prod.* **2023**, *194*, 116259.
[29] W. L. Lim, A. A. N. Gunny, F. H. Kasim, S. C. Gopinath, N. H. I. Kamaludin, D. Arbain, *Cellulose.* **2021**, *28*, 6183.
[30] Q. Liu, T. Yuan, Q.-J. Fu, Y.-Y. Bai, F. Peng, C.-L. Yan, *Cellulose.* **2019**, *26*, 9447.
[31] S. Hong, Y. Song, Y. Yuan, H. Lian, H. Liimatainen, *Ind. Crops Prod.* **2020**, *143*, 111913.
[32] S. Liu, Q. Zhang, S. Gou, L. Zhang, Z. Wang, *Carbohydr. Polym.* **2021**, *251*, 117018.
[33] A. Daneshfar, H. S. Ghaziaskar, N. Homayoun, *J. Chem. Eng. Data.* **2008**, *53*, 776.
[34] B. Soares, D. J. P. Tavares, J. L. Amaral, A. J. D. Silvestre, C. S. R. Freire, J. A. P. Coutinho, *ACS Sustain. Chem. Eng.* **2017**, *5*, 4056.
[35] Y. Song, X. Shi, S. Ma, X. Yang, X. Zhang, *Cellulose.* **2020**, *27*, 8301.
[36] K. H. Kim, T. Dutta, J. Sun, B. Simmons, S. Singh, *Green Chem.* **2018**, *20*, 809.
[37] H. Malaeke, M. R. Housaindokht, H. Monhemi, M. Izadyar, *J. Mol. Liq.* **2018**, *263*, 193.
[38] Y. Wang, H. Liu, X. ji, Q. Wang, Z. Tian, *Int. J. Biol. Macromol.* **2023**, *245*, 125227.
[39] H. Ren, C. Chen, Q. Wang, D. Zhao, S. Guo, *Bio. Res.* **2016**, *11*, 5435.
[40] A. P. Abbott, D. Boothby, G. Capper, D. L. Davies, R. K. Rasheed, *J. Am. Chem. Soc.* **2004**, *126*, 9142.
[41] L. Segal, J. J. Creely, A. E. Martin, C. M. Conrad, *Text. Res. J.* **1959**, *29*, 786.
[42] T. Tenhuen, A. Lewandowska, H. Orelma, L. Johansson, T. Virtanen, A. Harlin, M. Osterberg, S. Eichhorn, T. Tammelin, *Cellulose.* **2018**, *25*, 137.
[43] S. Y. Park, J. Y. Kim, H. J. Youn, J. W. Choi, *Int. J. Biol. Macromol.* **2018**, *106*, 793.
[44] Y. Zhao, D. G. Truhlar, *Theor. Chem. Acc.* **2008**, *120*, 215.
[45] M. J. Frisch, G. W. Trucks, H. B. Schlegel, G. E. Scuseria, M. A. Robb, J. R. Cheeseman, G. Scalmani, V. Barone, G. A. Petersson, H. Nakatsuji, X. Li, M. Caricato, A. V. Marenich, J. Bloino, B. G. Janesko, R. Gomperts, B. Mennucci, H. P. Hratchian, J. V. Ortiz, A. F. Izmaylov, J. L. Sonnenberg, D. Williams-Young, F. Ding, F. Lipparini, F. Egidi, J. Goings, B. Peng, A. Petrone, T. Henderson, D. Ranasinghe, et al. Gaussian 16 Revision A.03, Wallingford, **2016**.
[46] a) F. M. Bickelhaupt, K. N. Houk, *Angew. Chem., Int. Ed.* **2017**, *56*, 10070; b) F. M. Bickelhaupt, E. J. Baerends, in *Review Computer Chemistry*, (Ed.: K. B. Lipkowitz, D. B. Boyd), Wiley, Indianapolis **2000**, pp. 1–86.
[47] a) G. te Velde, F. M. Bickelhaupt, E. J. Baerends, C. Fonseca Guerra, S. J. A. van Gisbergen, J. G. Snijders, T. Ziegler, *J. Comput. Chem.* **2001**, *22*, 931; b) ADF2019, SCM. Theoretical Chemistry, Vrije Universiteit, Amsterdam: The Netherlands, https://www.scm.com/, (Accessed: July **2024**).
[48] E. van Lenthe, E. J. Baerends, J. G. Snijders, *J. Chem. Phys.* **1994**, *101*, 9783.
[49] a) M. Bortoli, S. M. Ahmad, T. A. Hamlin, F. M. Bickelhaupt, L. Orian, *Phys. Chem. Chem. Phys.* **2018**,*20*, 27592; b) L. Orian, W. J. Zeist, F. M. Bickelhaupt, *Organometallics.* **2008**, *27*, 4028; c) T. Scattolin, I. Pessotto, E. Cavarzerani, V. Canzonieri, L. Orian, N. Demitri, C. Schmidt, A. Casini, E. Bortolamiol, F. Visentin, F. Rizzolio, S. P. Nolan, *Eur. J. Inorg. Chem.* **2022**, *16*, e202200103.